Two-dimensional phononic crystals studied using a variational method: Application to lattices of locally resonant materials

Cécile Goffaux* and José Sánchez-Dehesa
Departamento de Física Teórica de la Materia Condensada, Universidad Autonomá de Madrid, E-28049 Madrid, Spain
(Received 19 October 2002; published 2 April 2003)

A variational method is introduced to study the propagation of elastic waves in two-dimensional periodic systems. First, it has been applied to a binary system consisting of an array of high-density cylinders in an epoxy background, where the advantages of the method are pointing out in regard with the well-known plane-wave expansion formalism. Second, a comprehensive study is performed for the two-dimensional counterpart of the ternary systems recently studied by Liu *et al.* [Z. Liu *et al.*, Science **289**, 1734 (2000)]. Numerical simulations predict that subfrequency gaps also appear because of the soft polymer that coats the cylinders. A simple mechanical model is introduced to give a physical insight of the phenomenon responsible for our findings.

DOI: 10.1103/PhysRevB.67.144301 PACS number(s): 43.40.+s, 41.20.Jb, 42.25.Fx

I. INTRODUCTION

The last decade has witnessed an increasing interest for the propagation of classical waves in periodic structures. Famous realizations are photonic crystals.[1] For these new crystals, both theoretical predictions and experiments have shown the appearance of frequency gaps for the propagation of electromagnetic waves, which has been used for the achievement of new optical devices.

Quickly, those studies were extended to the propagation of elastic and acoustic waves in periodic structures made of materials with different elastic properties, which have been named phononic crystals (PC's).[2–7] These new materials can be of real interest, since a large contrast between the elastic parameters is allowed. For example, systems composed of solid inclusions in a fluid are good candidates in order to obtain large gaps, which can lead to promising applications as a wide noise insulation.[7–11] Besides, their properties in the transmission bands have been used to build refractive devices such as lenses and acoustic interferometers.[12] On the other hand, more sophisticated combinations such as fluids infiltrated in a drilled solid[13,14] or solid-solid systems[15,16] have been demonstrated to produce full phononic band gap for ultrasounds.

Several theoretical methods have already been developed in order to study the elastic response of PC's. Mostly, the calculations are based on the plane-wave expansion (PWE) method, in which the wave equations are solved in the Fourier space.[17] Nevertheless, PC's involving media with a large contrast in their elastic properties are not easy to treat with PWE because a large number of plane waves is required to obtain reliable band structures, and unphysical flat frequency bands can appear. Other methods such as multiple scattering[10,18–21] or the finite-difference algorithms[22,23] overcome those difficulties.

In this work, we present a variational method (VM) that offers an alternative procedure to compute the band structure of PC's. As a numerical example of its strength, first, we have analyzed a two-dimensional (2D) system of Au cylinders periodically embedded in epoxy. It will be shown that the VM can improve the PWE technique because of its faster convergence and lower computational times. In regards with the algorithms based on multiple scattering theory (MST) and finite difference time domain (FDTD), these techniques are more suitable to treat the transmission/reflectance problem in finite structures and their comparison with the variational approach is out of scope of the present work. However, our experience in dealing with those techniques[24,25] indicates that the calculations of the phononic band structure present several drawbacks from the computational point of view. Thus, the technique based on FDTD requires a very strong reduction of the discretization steps, while the technique based on MST requires a large number of terms in the multipole expansion.

The pioneering work of Liu *et al.*[26] has motivated the second application of the VM. The authors studied three-dimensional (3D) PC's consisting of cubic arrays of coated spheres (the coating was a thin film of a soft material) immersed in an epoxy matrix. They predicted the appearance of a gap in a frequency range of two orders of magnitude lower than the one resulted by Bragg scattering. The origin of this phenomenon has been explained as due to the localized resonances associated with each scattering unit (the coated spheres).[26,27] Here, we employed the VM to analyze its 2D counterpart, i.e., lattices of coated cylinders in epoxy. Previously, this system has allowed us to describe the resonance features in the transmission spectra through finite structures as a result of a Fano-like interference phenomenon.[29] Our analysis shows that the properties of the 2D systems are comparable to the 3D structures, though some differences are observed. Finally, a simple mechanical model that uses springs, masses, and pendula has been employed as a mechanical analog that allows the understanding of the mechanism of band-gap formation as well as its dependence on parameters such as the lattice parameter.

The paper is organized as follows. Section II describes the main ingredients of the VM, which is applied to a binary system in Sec. III, where a comparison with the results obtained with the PWE is performed. In Sec. IV the system of coated cylinders is solved and discussed in terms of the known results in the 3D counterpart. Section V presents a

mechanical analog that allows an intuitive understanding of the previous results and, finally, Sec. VI summarizes the work.

II. THE VARIATIONAL METHOD

The wave propagation in an homogeneous solid can be strongly altered by inserting periodical inclusions of a solid compound with different elastic parameters. The periodic inclusions induce a wave scattering and destructive interferences can appear in some frequency ranges, leading to forbidden band gaps. Total reflection is then expected in these frequency ranges. Moreover, the vectorial character of the elastic displacement induces a strong coupling between the shearing and the longitudinal motions. Therefore, the study of how the modes propagate in these structures is not straightforward.

For 2D periodic systems, a partial decoupling of the elastic motion is obtained by assuming that the $\vec{k}$-wave vector of the incident waves is contained in the plane normal to the cylinder axis, which is taken as the z axis by definition. Thus, a pure transverse motion is found along this direction u_z. This is decoupled from that taking place in the normal plane u_i $(i=1,2)$. The equations describing these distinct displacements can be expressed in the harmonic approximation by

$$-\rho(\mathbf{r})\omega^2 u_z(\mathbf{r}) = \boldsymbol{\nabla}\cdot[\mu(\mathbf{r})\boldsymbol{\nabla} u_z(\mathbf{r})], \tag{1}$$

$$-\rho(\mathbf{r})\omega^2 u_i(\mathbf{r}) = \frac{\partial}{\partial x_i}[\lambda(\mathbf{r})\boldsymbol{\nabla}\cdot\mathbf{u}(\mathbf{r})] + \boldsymbol{\nabla}\cdot[\mu(\mathbf{r})\boldsymbol{\nabla} u_i(\mathbf{r})] + \boldsymbol{\nabla}\cdot\left[\mu(\mathbf{r})\frac{\partial}{\partial x_i}\mathbf{u}(\mathbf{r})\right] \quad (i=1,2), \tag{2}$$

where $\mathbf{r}=(x_1,x_2)$ represents a position vector in the plane of the periodicity, $\boldsymbol{\nabla}$ is the 2D differential operator, $\rho(\mathbf{r})$ is the mass density distribution, and $\mu(\mathbf{r})$ and $\lambda(\mathbf{r})$ are the space-dependent Lamé coefficients.

The usual method employed to solve Eqs. (1) and (2) uses a PWE of the parameters inside the unit cell. Afterwards, the Bloch theorem is used to account for the periodicity of the crystal. For a set of n_g plane waves, the problem is reduced to a matrix generalized eigenvalue problem. Fast computational routines exist that allow to obtain the eigenmodes of the system by diagonalizing matrices of dimension $n_g\times n_g$ or $2n_g\times 2n_g$ according to the case, Eq. (1) or Eq. (2), respectively.

A solution of the equivalent problem for fluid systems was previously solved in the direct space.[8] Here, the same strategy is followed, and we formulate its version extended to the case of elastic composites. Briefly, the method expands the elastic displacements in a set of N^2 localized basis functions with a functional form that satisfies the Bloch theorem:

$$u_z(\mathbf{r}) = \sum_{\ell}^{N^2} c_z^{\ell} \sum_{R} e^{i\mathbf{k}\cdot\mathbf{R}}\phi_\ell(\mathbf{r}-\mathbf{R}) = \sum_{\ell}^{N^2} c_z^{\ell}\Phi_\ell(\mathbf{r}), \tag{3}$$

$$u_i(\mathbf{r}) = \sum_{\ell}^{N^2} c_i^{\ell} \sum_{R} e^{i\mathbf{k}\cdot\mathbf{R}}\phi_\ell(\mathbf{r}-\mathbf{R}) = \sum_{\ell}^{N^2} c_i^{\ell}\Phi_i(\mathbf{r}) \quad (i=1,2), \tag{4}$$

where $\mathbf{k}$ is a 2D wave vector contained in the first Brillouin Zone (BZ) of the reciprocal lattice and $\phi_\ell(\mathbf{r})$ are the localized basis set. Each function in the set is a product of two one-dimensional cubic splines (i.e., piecewise C^2-smooth cubic polynomials,[30]) which is centered at the N^2 nodes of a 2D grid defined in each unit cell of the lattice.

Inserting the expansions of Eqs. (3) and (4) in Eqs. (1) and (2) and making the projections on each function $\phi_k(\mathbf{r})$, the following generalized eigenvalue problem is obtained:

$$G^{\ell,k}c_z^{\ell} = -\omega^2 P^{\ell,k}c_z^{\ell}, \tag{5}$$

$$H_{i,j}^{\ell,k}c_j^{\ell} = -\omega^2 S_{i,j}^{\ell,k}c_j^{\ell} \quad (i,j=1,2;\ell,k=1,N^2). \tag{6}$$

This leads to a $2N^2\times 2N^2$ matrix problem for the in-plane motions and a $N^2\times N^2$ problem for the out-plane motions. The matrix elements are

$$G^{\ell,k} = \int_{cell}\phi_k(\mathbf{r})\boldsymbol{\nabla}\cdot[\mu(\mathbf{r})\boldsymbol{\nabla}\Phi_\ell(\mathbf{r})]d\mathbf{r} = \sum_R e^{i\mathbf{k}\cdot\mathbf{R}}g^{\ell,k}, \tag{7}$$

$$P^{\ell,k} = \int_{cell}\phi_k(\mathbf{r})\rho(\mathbf{r})\Phi_\ell(\mathbf{r})d\mathbf{r} = \sum_R e^{i\mathbf{k}\cdot\mathbf{R}}p^{\ell,k}, \tag{8}$$

$$H_{i,j}^{\ell,k} = \int_{cell}\phi_k(\mathbf{r})\frac{\partial}{\partial x_i}\left[\lambda(\mathbf{r})\frac{\partial\Phi_\ell(\mathbf{r})}{\partial x_j}\right]d\mathbf{r} + \int_{cell}\phi_k(\mathbf{r})\frac{\partial}{\partial x_j}\left[\mu(\mathbf{r})\frac{\partial\Phi_\ell(\mathbf{r})}{\partial x_i}\right]d\mathbf{r} \tag{9}$$

$$+\int_{cell}\phi_k(\mathbf{r})\boldsymbol{\nabla}\cdot[\delta_{ij}\mu(\mathbf{r})\boldsymbol{\nabla}\Phi_\ell(\mathbf{r})]d\mathbf{r} = \sum_R e^{i\mathbf{k}\cdot\mathbf{R}}h^{\ell,k}, \tag{10}$$

$$S_{i,j}^{\ell,k} = \int_{cell}\phi_k(\mathbf{r})\delta_{ij}\rho(\mathbf{r})\Phi_\ell(\mathbf{r})d\mathbf{r} = \sum_R e^{i\mathbf{k}\cdot\mathbf{R}}s^{\ell,k}, \tag{11}$$

where $g^{\ell,k}$, $p^{\ell,k}$, $h^{\ell,k}$, and $s^{\ell,k}$ are elements that can be cast into integrals involving localized cells in the unit cell located at the origin of coordinates. Note that the method is variational with respect to the c_i or c_z coefficients. Thus, the convergence is achieved when a sufficient number of basis functions is employed in Eqs. (3) and (4).

As for photonic crystals,[1] a variational principle exists and the solutions can be thought to be the functions that minimize the functional $E_f[u_i]$, $E_f[u_z]$, associated, respectively, with the elastic problem describing the in-plane and out-of-plane motions:

$$E_f[u_z]=\frac{1}{2}\frac{\int_{cell}\mu(\mathbf{r})|\nabla u_z(\mathbf{r})|^2\mathbf{dr}}{\int_{cell}\rho(\mathbf{r})|u_z(\mathbf{r})|^2\mathbf{dr}}; \tag{12}$$

$$E_f[u_i]=\frac{1}{2}\frac{\int_{cell}\lambda(\mathbf{r})|\nabla\cdot\mathbf{u}(\mathbf{r})|^2\mathbf{dr}+\sum_{i=1}^{2}\int_{cell}\mu(\mathbf{r})\left[\left|\nabla u_i(\mathbf{r})\right|^2\mathbf{dr}+\sum_{j=1}^{2}\frac{\partial u_j(\mathbf{r})}{\partial x_i}\frac{\partial u_i(\mathbf{r})}{\partial x_j}\right]\mathbf{dr}}{\int_{cell}\rho(\mathbf{r})|\mathbf{u}(\mathbf{r})|^2\mathbf{dr}} \quad (i=1,2). \tag{13}$$

III. RESULTS FOR A BINARY SYSTEM: AU CYLINDERS IN EPOXY

The parameters that induce the appearance of a gap in binary systems are the filling fraction, the lattice symmetry, the topology of the scatterers, and the contrast between elastic properties of materials.[4,31,32] The density contrast plays a fundamental role; inserting very high-density inclusions in a light host (*cermet* topology)[4] is the more efficient way of obtaining wide gaps.

Here, as a test example for the VM, we consider an hexagonal lattice of Au cylinders in epoxy. Figure 1 shows the dispersion relations of the elastic modes corresponding to a crystal having a filling fraction $f_h=\pi/2\sqrt{3}(d/a)^2=0.79$, where d is the diameter of cylinders and a is the lattice constant. The elastic parameters employed in the calculations were $\rho_{gold}=19\,500\ \mathrm{kg\,m^{-3}}$, $\rho_{epo}=1180\ \mathrm{kg\,m^{-3}}$, $c_{l,gold}=3360\ \mathrm{m\,s^{-1}}$, $c_{l,epo}=2535\ \mathrm{m\,s^{-1}}$, $c_{t,gold}=1239\ \mathrm{m\,s^{-1}}$, $c_{t,epo}=1157\ \mathrm{m\,s^{-1}}$. The modes propagating in the plane (full lines) as well as those propagating along the z direction (dotted lines) were computed with the variational method by employing 32 nodes in each direction of the unit cell. The results obtained with the PWE method by using a set of 960 PW are represented by the square (in-plane modes) and the triangular (out-of-plane modes) symbols. A good agreement is found between the two methods. A gap separates the dispersion curves of the in-plane modes as well of the pure transverse ones. A complete gap, resulting from the superposition of the two band structures, settles between the fourth and the fifth bands at a midgap frequency of about 0.60 reduced units.

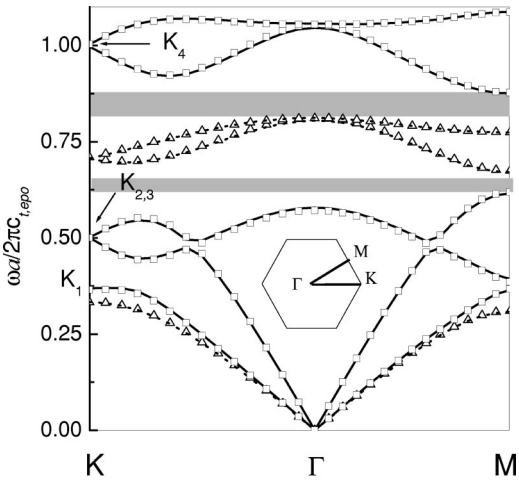

FIG. 1. Phononic band structure along the two high-symmetry directions of the Brillouin Zone (see inset) for an hexagonal lattice of Au cylinders embedded in epoxy. The filling fraction is 0.79. The continuous (dotted) lines represent the in-plane (out-of-plane) modes computed with the variational method. The symbols represent the results obtained by using a plane-wave expansion method. The shadowed regions define the complete gaps. The frequencies ω are given in reduced units, a is the lattice constant, and $c_{t,epo}$ is the transverse velocity inside the epoxy.

The analysis of the band structures in Fig. 1 is straightforward for the case of pure transverse modes u_z because their dispersion relations are the solution of a simple scalar equation, Eq. (1). The gaps are the consequence of a destructive interference of the wave scattered in the periodic system. The order of magnitude of the midgap frequency ω_g, can be estimated. Its value should be closer to the frequency where the band folding takes place (i.e., at the borders of the first BZ), and this frequency is calculated by using an empty lattice approach. For example, the estimation of the midgaps for the transversal modes is made as follows,

$$\omega_g(M)\approx c_{t,epo}k_M=\frac{2\pi c_{t,epo}}{\sqrt{3}a}=0.57\frac{2\pi c_{t,epo}}{a},$$

at the M point; (14)

$$\omega_g(K)\approx c_{t,epo}k_K=\frac{4\pi c_{t,epo}}{3a}=0.66\frac{2\pi c_{t,epo}}{a},$$

at the K point, (15)

where $k_{M,K}=|\vec{k}_{M,K}|$. The values (in reduced units) roughly agree with the actual ones resulting from the band-structure calculation, 0.49 and 0.52 for the M and K points, respectively. This result points out that the gaps created by a Bragg scattering mechanism appear at frequencies related to the lattice periodicity. So, gap openings at very low frequencies only can be achieved by using very large structures or very low transverse velocity in the background. For example, a gap in the range of few Hertz can be achieved with this Au/epoxy system by using a lattice parameter of the order of several hundred meters. Another parameter of interest in con-

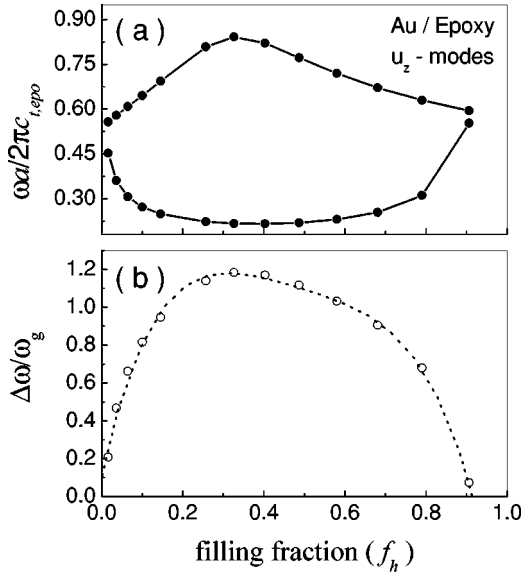

FIG. 2. (a) The edges determining the gap in an hexagonal lattice of Au cylinders in epoxy for several filling fractions (f_h). (b) The corresponding normalized gap width is ($\Delta\omega/\omega_g$), where ω_g is the midgap frequency.

trolling the band gap is the filling fraction *f*. Figures 2(a) and 2(b) show, respectively, the band edges of the first gap and its normalized width for the modes u_z. These results represent typical behaviors associated with a Bragg gap. Particularly, a Bragg gap peaks at some intermediate filling fraction. Thus, Fig. 2(b) shows that at $f_h \approx 0.32$ the normalized gap width is maximum.

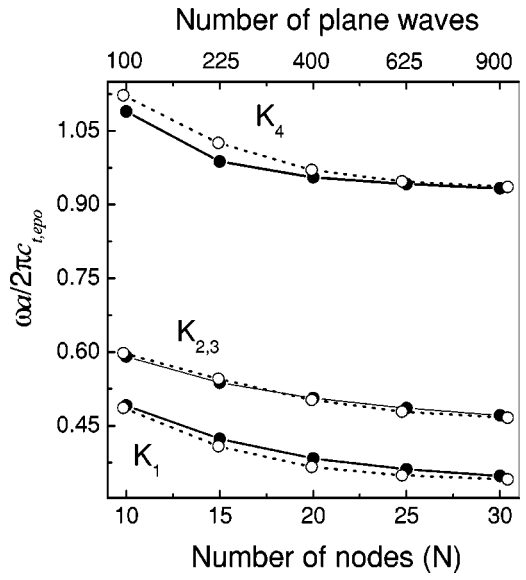

FIG. 3. Convergence of the lower four in-plane frequencies for both variational (continuous lines) and plane-wave expansion methods (dotted lines). They correspond to the points K_1, $K_{2,3}$ and K_4 in Fig. 1. The top axis representing the number of plane-waves employed in the plane-wave calculation is aligned with the number of nodes in the bottom axis that produces a matrix having the same dimension as in the variational method.

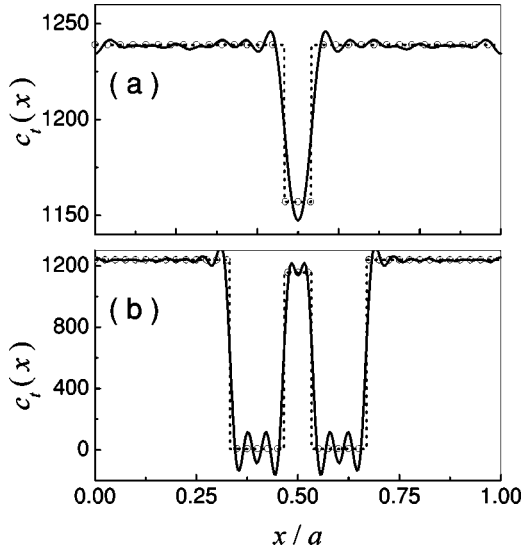

FIG. 4. (a)The transverse velocity $c_t(x)$ along a line joining two cylinders in a lattice of Au cylinders in epoxy. The coordinate (in units of the lattice constant, a) begins at the center of one cylinder and ends at the center of one of its neighbors. The plane-wave representation (continuous line) shows quite important oscillations near the Au/epoxy interfaces. The variational method (white circles) presents in a more accurate way the exact interfaces (dotted line). (b) The corresponding plot for the case of Au cylinders coated with polymer in a epoxy host.

The convergence of the VM and the PWE method are compared in Fig. 3. The behavior of the lower four frequencies of the in-plane modes at the *K* point (points K_1,$K_{2,3}$, and K_4 in Fig. 1) is shown as a function of the number *N* of grid points employed along each direction in the unit cell. For the PWE calculations we made a similar study and have changed the number of plane waves, from 97 to 925. The two abscissa scales are aligned in such a way that the size of the matrices are the same in both methods. From Fig. 3 it is noticeable that the three lower frequencies, K_1 and $K_{2,3}$, converge similarly in both methods. However, the VM improves the convergence of the higher mode K_4. This improvement can be understood from Fig. 4(a), which shows the behavior of the transverse velocity c_t along the line joining two neighbor cylinders. The PWE method (solid line) employed 960 functions to reproduce the speed discontinuity with some accuracy, while the VM (hollow circles) used 32 nodes. In comparison with the exact behavior (dotted line), the result from the PWE method shows the well-known Gibbs oscillations at the interfaces, which are the origin of the lower convergence at high frequencies. In an opposite way, the VM that works in the direct space seems to describe the interfaces more correctly, which justifies its faster convergence. Another improvement of the VM comes from the spatially localized character of the spline basis. This property decreases the computational time for various reasons: (i) The constructions of the matrices in Eqs. (7)–(11) can be performed in two steps; the first one allows to get the common part of the matrix elements, which, in the second step, are calculated by multiplying the Bloch factors; and (ii) the localized character of the functions leads to sparse matrices,

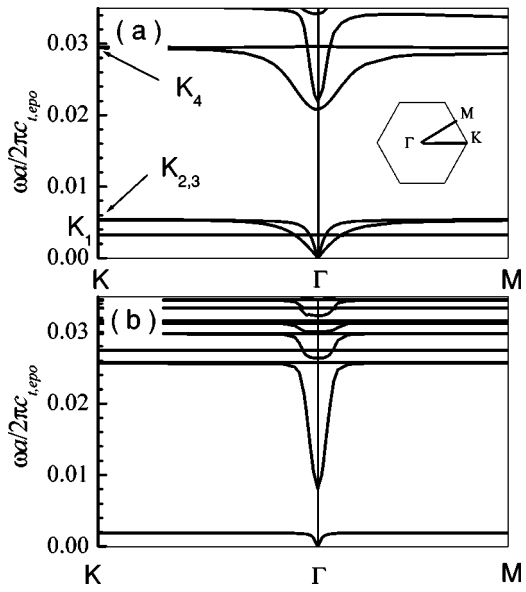

FIG. 5. (a) Band structure of the in-plane modes existing in an hexagonal lattice of coated cylinders in epoxy. (b) Band structure of the corresponding out-of-plane modes. The filling fraction of the lattice is 0.79. The variational calculation employed 40 localized functions. The complete flat bands are associated with modes localized in the coating layer (see Fig. 8).

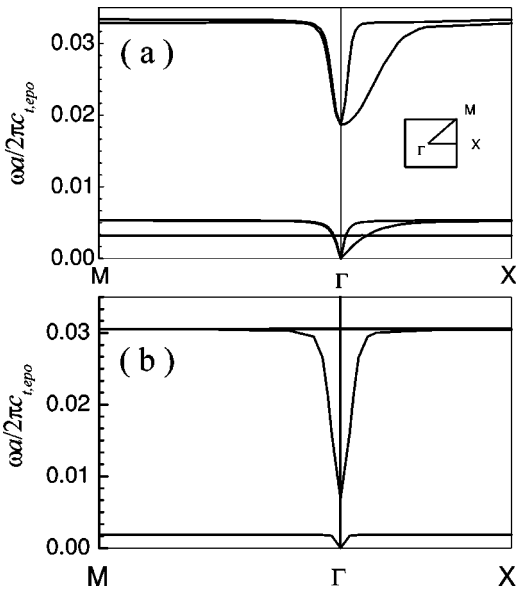

FIG. 6. (a) Band structure of the in-plane modes existing in a square lattice of coated cylinders in epoxy. (b) Band structure of the corresponding out-of-plane modes. The filling fraction of the lattice is 0.68. The variational calculation employed 40 localized functions. The complete flat bands are associated with modes localized in the coating layer.

which are solved by designed routines that substantively reduce the diagonalization time.

IV. RESULTS FOR LATTICES OF LOCAL RESONATORS: COATED CYLINDERS IN EPOXY

Very soft polymers were recently used[26] as the coating of Pb spherical inclusions arranged in a simple cubic lattice in an epoxy host. The very low transverse velocity of the coating layer resulted in a strong resonant band structure with a gap at a frequency of two orders of magnitude lower than the expected one by Bragg scattering. In analogy with electromagnetic situations in which the dielectric function can be negative, this phenomenon was interpreted as the consequence of effective negative elastic constants in the range of frequencies where the subfrequency gaps appear.

Here, we analyzed the effects produced by adding a thin layer of soft polymer to the binary 2D-PC studied in Sec. II. Thus, we coat Au cylinders with a thin layer of rubber polymer, whose elastic parameters are $\rho_{pol}=1300\ \mathrm{kg\,m^{-3}}$, $c_{l,pol}=33\ \mathrm{m\,s^{-1}}$, $c_{t,pol}=5\ \mathrm{m\,s^{-1}}$. In order to compare the band structures in Fig. 1, we keep the same external radius for the cylinders and for the same lattice constant. As the ratio between the core radius r_{core} (Au cylinder) and the external radius r_{ext} (Au+coating) we use 0.71. Figure 5 presents the band structures corresponding to coated cylinders in an hexagonal lattice.

For sake of comparison and discussion, Fig. 6 presents the results corresponding to the same cylinders arranged in a square lattice. In this case, equal external radius and lattice parameter produce a slightly lower filling fraction, which in this lattice is $f_s=\pi(r_{ext}/a)^2=0.68$.

The convergence of the VM has also been analyzed and compared with the PWE method. The behavior of frequencies at K_1, $K_{2,3}$, and K_4 points is presented in Fig. 7 as a function of the basis-set employed. It is shown that both methods have a very low convergence in comparison with the results obtained for binary structures, especially at higher frequencies. Forty nodes and 1600 plane waves, respectively, are needed in order to guarantee convergence better than 5%. This low convergence is due to the high contrast between the

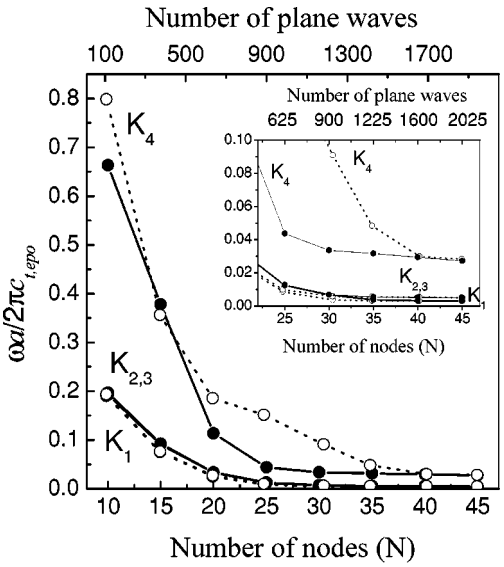

FIG. 7. Study of the convergence of in-plane modes for both plane-wave and variational methods. Four modes were analyzed at the K point of the Brillouin zone, denoted by K_1, $K_{2,3}$, and K_4. The inset shows a zoom of the total graph in the low-frequency region.

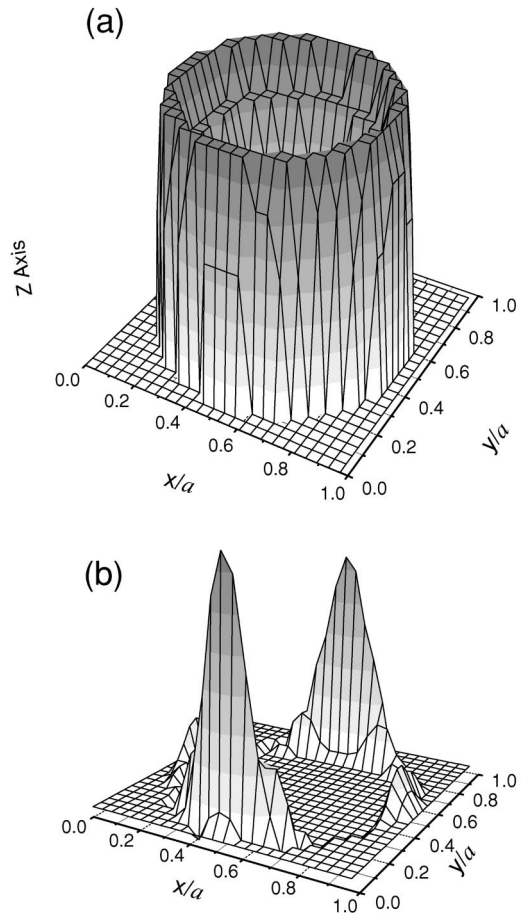

FIG. 8. (a) Modulus of the displacement vector $|\mathbf{u}(x,y)|$ for the in-plane modes associated to the first flat band in Fig 6. (b) the same magnitude calculated for the modes at the second flat band. The axis is given in reduced units (a is the lattice parameter). In both cases the displacement occurs inside the polymer layer (see text).

elastic parameters of the coating and the other two materials, which requires to introduce a large basis function set in the VM calculations, or equivalently a large number of Fourier components in the PWE method. As in the binary case, the VM converges faster at high frequencies, because it represents the sharp interfaces more exactly [see Fig. 3(b)]. In the extreme case of a 2D-PC having one medium of zero transversal velocity, as in a fluid, both methods have the same numerical problems regarding worse convergence and unphysical flat bands appearing in the dispersion relations. These drawbacks are related to the diagonalization procedure, since they do not appear in other numerical algorithms.

Regarding the band structures shown in Figs. 5 and 6, the it is remarkable the presence of flat bands crossing the complete BZ. These flat bands are real bands and they are converged. They are associated with eigenmodes of the soft polymer as it is shown in Fig. 8, where the elastic displacements $|\mathbf{u}(x,y)|$ associated with the in-plane modes of two different flat bands in Fig. 6 are represented. Figures 8(a) and 8(b) plot the modes associated with the flat bands with frequencies (in reduced units) 0.0032 and 0.027, respectively. Both are eigenmodes localized inside the polymer coating.

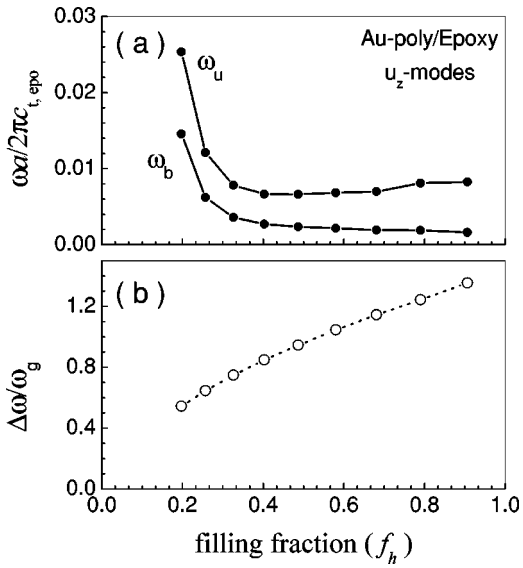

FIG. 9. (b) The band edges determining the first gap of the out-of-plane modes in the hexagonal lattice of coated cylinders in epoxy for several filling fractions (f_h). (b) Behavior of the corresponding normalized gap width resulting from (a).

The very low transverse velocity of the coating allows for the modes to propagate at very low frequencies. Flat bands also appear in binary systems if the cylinders are filled with a material elastically softer than the matrix, and the elastic vibrations are localized inside the cylinders.[23]

The most noticeable feature in Figs. 5 and 6 is the appearance of a complete gap in a frequency region two orders of magnitude lower than the expected one by the Bragg conditions [see Eqs. (14) and (15)]. This subfrequency gap is originated from the resonances arising from the insertion of a soft coating, as was pointed out by Liu and co-workers[26,27] studying the 3D systems. On the other hand, the band structure is sensitive to the lattice symmetry: the hexagonal lattice shows a symmetric dispersion relation around the Γ point, while the square lattice shows a dependency on the $\vec{k}$-wave vector. Moreover, we found that, for an equivalent filling fraction, the size of the subfrequency gaps are larger for the hexagonal case. These two last properties are well-known results for gaps having a Bragg origin. Particularly, the larger gap obtained for the hexagonal lattice is due to the higher coordination number of the hexagonal lattice that makes stronger the total interaction between neighbor resonances. Therefore, the band structure of these ternary systems show a mixed character: it presents subfrequency gaps produced by the localized states existing at the cylinders positions, but these gaps behave in a similar manner as the Bragg gaps if one studies their dependence with symmetry due to the weak interaction between the localized states.

In order to support the resonant origin of the subfrequency gaps, we plot in Fig. 9 the dependency on f_h of the band edges determining the lowest gap for the out-of-plane modes and the resulting normalized gap for the case of the hexagonal lattice. The lattice parameter a is kept constant as well as the ratio $r_{ext}/r_{core} \approx 1.4$; only r_{ext} changes. The behavior of the band edges is completely different to that char-

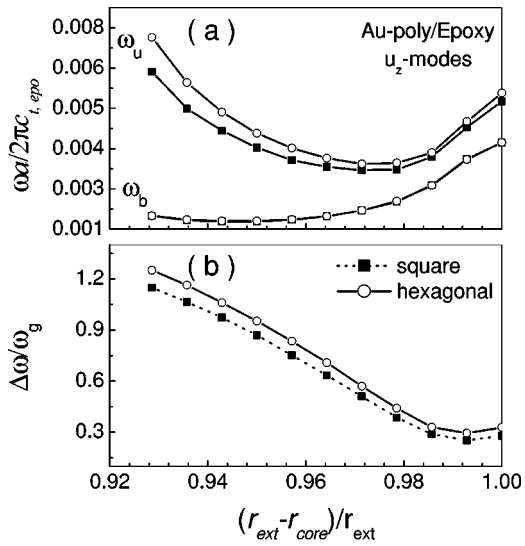

FIG. 10. (a) Dependence of the coating thickness of the band edges determining the lowest subfrequency gap obtained for a lattice of coated cylinders in epoxy. The hexagonal and square lattices are studied. r_{ext} and the lattice parameter are fixed, only r_{core} changes. (b) Behavior of the corresponding normalized gap width.

acterizing a Bragg gap (see, for example, Fig. 2). The upper panel shows that both edges quickly converge to values that change slowly with f_h. This is a signature of their resonant origin. Particularly, the pinning of the bottom edge, ω_b, is a consequence of the strong localized character of its associated mode, which consists of a vibration of the Au inner core. The upper edge, ω_u, changes slightly due to the mixed character of its mode, where the epoxy is also involved. The small changes in frequency are a consequence of the increasing resonances' interaction produced by the decreasing distance between cylinders.

Figures 10(a) and 10(b) present a further support of the last conclusion. Figure 10(a) shows the influence of the coating thickness on the frequency edges determining the first subfrequency gap in two different lattices: the hexagonal and the square. The lower edge for the hexagonal (square) lattice is calculated at the *K* point (*X* point), and the upper edge is taken at the Γ point. The lattice constant is the same in both lattices and is a constant along the calculations. Notice that both lattices behave similarly. The lower edges are the same in both lattices, which indicates its strongly localized character (associated to the vibration of the Au core). On the other hand, the upper edge in both lattices slightly depends on the coating thicknesses and the lattice symmetry. As stressed previously, this behavior is due to the mixed character of the mode at Γ point, which explains its sensitivity to *f* and the lattice symmetry. Also notice that in the absence of Au core ($r_{core}=0$) the subfrequency gap still exists. Finally, Fig. 10(b) shows the behavior of the normalized gap. It is large in the hexagonal lattice because of its higher *f*. Also, this plot demonstrated that the presence of a soft material guarantees the presence of a subfrequency gap even in binary systems.

It must be stressed that similar phenomenon can appear under the presence of surface waves on the cylinder units. An electromagnetic analog of this effect is the case of surface plasmons on metallic arrays of cylinders or spheres, where the appearence of minigaps in the photonic band structures has been demonstrated.[28]

V. A MECHANICAL ANALOG

In many cases, mechanical analogies are helpful in order to understand the physical mechanisms producing some features in the spectra of complicate systems, being these elastic or electromagnetic. Thus, in a recent work[29] we used a 1D mechanical model of masses and springs to clarify the origin of the asymmetric peaks observed in the transmission spectra across a finite slab made of coated cylinders. Beautiful examples of mechanical analogies can be found in many textbooks.[33]

Here, we introduce a simple model in order to get a physical insight regarding the gap formation by the presence of localized resonances at the coated cylinders. It is based on a model initially described by J.J. Thomson and constructed by J.H. Vincent[34] to illustrate Helmholtz's theory of dispersion. The model consists of a linear chain of masses *M* and springs with a stiffness constant K_s. Attached to each mass *M*, there exists a light pendulum (mass *m* and length *l*), which represents the localized mode associated with each cylinder in the exact elastic system. Gravity does not act over any of the masses *M*, because it is assumed that each mass is hanging from a long threat suspended from a plank fastened to the ceiling.

The mechanical system previously described has an analytical solution. The resulting band structure has two branches:

$$\omega_{\pm}^2(k)=\omega_p^2\frac{M+m}{M}+2\omega_0^2\sin^2\left(\frac{ka}{2}\right)\pm\omega_p^2\frac{M+m}{M}\sqrt{1+4\frac{\omega_0^4}{\omega_p^4}\left(\frac{M}{M+m}\right)^2\sin^4\left(\frac{ka}{2}\right)+4\frac{\omega_0^2}{\omega_p^2}\frac{M(M-m)}{(M+m)^2}\sin^2\left(\frac{ka}{2}\right)}, \quad (16)$$

where *k* is the wave vector, ω_p is the eigenfrequency of the pendulum ($\omega_p=\sqrt{g/\ell}$), and ω_0 is the eigenfrequency of the spring ($\omega_0=\sqrt{K_s/M}$). A gap appears between the maximum frequency of the first branch ω_- at the zone boundary (i.e., the bottom edge ω_b) and the lowest frequency of the second branch ω_+ at the Γ point (the upper edge ω_u). From Eq. (16), these frequencies are

$$\omega_b = \omega_-\left(\frac{\pi}{a}\right) = \left[\omega_p^2\frac{M+m}{M} + 2\omega_0^2 - \omega_p^2\frac{M+m}{M}\sqrt{1+4\frac{\omega_0^4}{\omega_p^4}\left(\frac{M}{M+m}\right)^2 + 4\frac{\omega_0^2}{\omega_p^2}\frac{M(M-m)}{(M+m)^2}}\right]^{1/2}, \tag{17}$$

$$\omega_u = \omega_+(0) = \omega_p\sqrt{\frac{2(M+m)}{M}}. \tag{18}$$

Figure 11 shows a schematic representation of the model (upper panel) and the corresponding dispersion relation (lower panel) calculated for a given set of parameters. Notice the good qualitative agreement with the exact dispersion relations of the 2D problem at low frequencies. In this simple model, the frequency ω_0 and the mass M are associated with the background, in which the localized states are embedded. ω_p defines the frequency of the resonant level attached to each cylinder and m defines its vibrating mass. These magnitudes can be used as fitting parameters to reproduce the dispersion relations in Figs. 5 and 6.

For example, let us consider the case of the first subfrequency gap for the out-of-plane modes in the hexagonal lattice represented in Fig. 5. First, ω_0 is determined from the dispersion relation of uncoated cylinders (see Fig. 1) by fitting the slope of the dispersion relation at low frequencies, since for the linear chain $\omega(k) = 2\omega_0|\sin(ka/2)|$. We obtained $\omega_0 \approx 0.112$ (in red. units). The mass of the pendulum is given by $m_L \approx \rho_{Au}\pi r_{core}^2 = 1531\ \mathrm{g\,m^{-1}}$, where it has been taken into account that the localized level is associated with a vibration of the Au core. We work with masses per unit length since we are dealing with a 2D system. ω_p can be easily obtained by using the simplifying assumption $\omega_0 \gg \omega_p$, which allows to cast Eq. (17) in $\omega_b \approx \sqrt{2}\omega_p$. Therefore, $\omega_p \approx 0.0013$ (red. units). Finally, the mass $M_L \approx 82\ \mathrm{g\,m^{-1}}$ has been fitted to reproduce ω_u. Figure 12(a) presents the dispersion relations (solid lines) that simulate the exact 2D system. The dispersion relations for the uncoupled systems are also represented (dotted lines) for comparison purposes, the flat line gives the level ω_p of an isolated localized state (the pendulum), and the linear curves starting at the origin give the dispersion relation of the background (the linear chain).

In order to test the mechanical model, we have analyzed

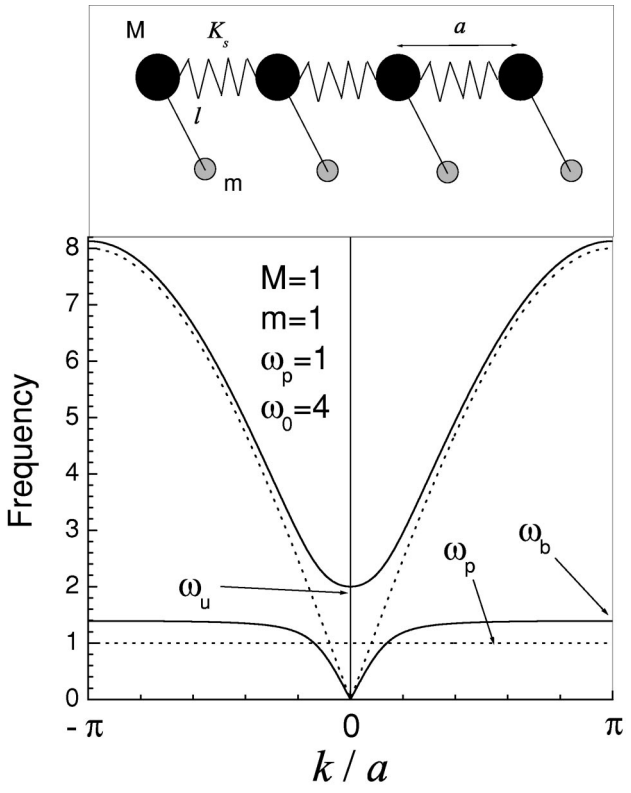

FIG. 11. (top) Schematic representation of the mechanical model employed to simulate the full elastic system of coated cylinders in epoxy. It consists of a string of masses (M) and springs (stiffness constant K_s). The periodicity is given by a. A pendulum (of length l and mass m) is attached to each mass M. (bottom) The solid lines represent the dispersion relations of a mechanical system defined by the given parameters. ω_b and ω_u define, respectively, the bottom and the upper edges of the gap. The dotted lines represent the frequency of the pendulum ω_p and the dispersion relation of the chain with no pendula attached.

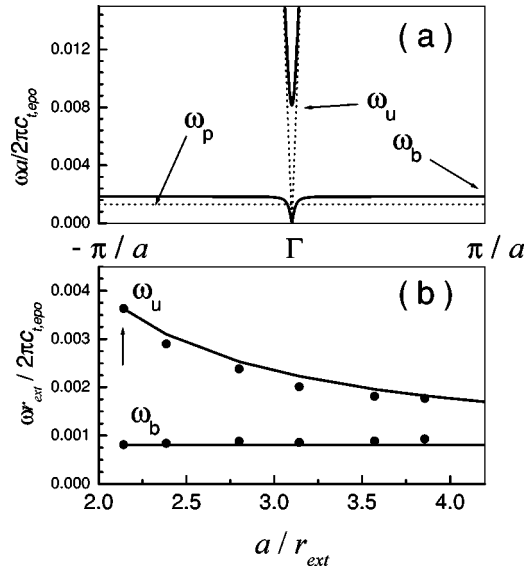

FIG. 12. (a) Dispersion relation for the out-of-plane modes shown in Fig. 5 fitted with the mechanical model of Fig. 11. (b) Behavior of the edges determining the first subfrequency gap in the hexagonal lattice of coated cylinders in epoxy for several lattice constants. The external radius and the core radius are kept constants. The symbols represent the variational calculation of the exact 2D system, and the solid lines define the results obtained with the model (see text).

how ω_b and ω_u depend on the lattice parameter. We have assumed that the mass M_L in Eq. (18) scales according to the volume outside the Au core; i.e., $M_L(a)=M_L(a_0)(\sqrt{3}/2a^2-\pi r_{core}^2)/(\sqrt{3}/2a_0^2-\pi r_{core}^2)$, where $M_L(a_0)$ is fitted. Regarding the exact 2D system, a set of 60 localized functions were used in the VM to obtain results fully converged. The results are shown in Fig. 12(b). It is observed that both systems, the exact (symbols) and the mechanical analog (solid line), behave similarly. First, the bottom edge does not change with the lattice because it is determined by the geometry of the local resonator that does not change the calculation. And second, the upper edge continuously decrease in agreement with the law predicted by the model [see Eq. (18)]. The monotic decreasing of the difference $\omega_u-\omega_b$, which gives an estimation of the interaction strength between the localized level and the continuum, indicates that the interaction strength decreases when the distance between resonances increases. In fact, in the limit of isolated resonaces $a\to\infty$ (i.e., when $M\gg m$), $\omega_u\to\omega_b$and the gap closes according to Eq. (18).

It can be concluded that the mechanical analog employed contains the main ingredients to get a physical insight of the mechanism leading to the formation of subfrequency gaps in elastic systems consisting of locally resonant units in a matrix.

VI. CONCLUSION

We have presented a variational method that works in the direct space and allows to compute the band structures of elastic crystals with two-dimensional periodicity. Arrays of gold cylinders displayed in an epoxy host were first studied to show its advantages in comparison with the plane-wave expansion method. We concluded that the variational method converges faster at high frequencies and it is computationally more effective. Second, the method were employed to study lattices of cylinders coated with a polymer tube to demonstrate that these systems allows to decrease the gap frequency by two orders of magnitude. The subfrequency gaps are attributed to resonant phenomena taking place in the cylinder units as it was previously shown in the 3D counterparts. Finally, we introduced a mechanical analog consisting of a string of springs, pendula, and masses that allows us to understand the physical mechanism of creation of such subfrequency gaps, as well as their sensitivity to different parameters as the lattice periodicity.

ACKNOWLEDGMENTS

This work was funded by the program *Bref séjour à l'étranger* of the *FNRS*. C. G. acknowledges the support of the *FIRST* program of the Walloon Region Government and the Research and Development Center of Cockerill-Sambre (Arcelor Group). We also acknowledge financial aid provided by the Spanish CICYT and the computing facilities provided by the *Centro de Computación Científica* at the UAM. We thank D. Caballero for his contribution in the code writing. Both authors acknowledge Ph. Lambin and F. Meseguer for their continuous support.

*Permanent address: Laboratoire de Physique du Solide, Facultés Universitaires Notre-Dame de la Paix, 61 rue de Bruxelles, B-5000 Namur, Belgium.

[1] J. D. Joannopoulos, R. D. Meade, and J. N. Winn, *Photonic Crystals* (Princeton University Press, Princeton, 1995).
[2] M.M. Sigalas and E.N. Economou, J. Sound Vib. **158**, 377 (1992).
[3] M.M. Sigalas and E.N. Economou, Solid State Commun. **86**, 141 (1993).
[4] E.N. Economou and M.M. Sigalas, Phys. Rev. B **48**, 13 434 (1993).
[5] M.S. Kushwaha, P. Halevi, L. Dobrzynski, and B. Djafari-Rouhani, Phys. Rev. Lett. **71**, 2022 (1993)
[6] M.S. Kushwaha, P. Halevi, G. Martínez, L. Dobrzynski, and B. Djafari-Rouhani, Phys. Rev. B **49**, 2313 (1994)
[7] R. Martínez-Sala, J. Sancho, J.V. Sánchez, V. Gómez, J. Llinares, and F. Meseguer, Nature (London) **378**, 241 (1995).
[8] J.V. Sánchez-Pérez, D. Caballero, R. Mártinez-Sala, C. Rubio, J. Sánchez-Dehesa, F. Meseguer, J. Llinares, and F. Gálvez, Phys. Rev. Lett. **80**, 5325 (1998).
[9] D. Caballero, J. Sánchez-Dehesa, C. Rubio, R. Mártinez-Sala, J.V. Sánchez-Pérez, F. Meseguer, and J. Llinares, Phys. Rev. E **60**, R6316 (1999).
[10] M. Kafesaki, R.S. Penciu, and E.N. Economou, Phys. Rev. Lett. **84**, 6050 (2000).
[11] C. Goffaux and J.P. Vigneron, Phys. Rev. B **64**, 075118 (2001).
[12] F. Cervera, L. Sanchis, J.V. Sanchez-Pérez, R. Martínez-Sala, C. Rubio, F. Meseguer, C. López, D. Caballero, and J. Sánchez-Dehesa, Phys. Rev. Lett. **88**, 023902 (2002).
[13] F.R. Montero de Espinosa, E. Jimenez, and M. Torres, Phys. Rev. Lett. **80**, 1208 (1998).
[14] M. Torres, F.R. Montero de Espinosa, and J.L. Aragon, Phys. Rev. Lett. **86**, 4282 (2001).
[15] J.O. Vasseur, P.A. Deymier, G. Frantziskonis, G. Hong, B. Djafari-Rouhani, and L. Dobrzynski, J. Phys.: Condens. Matter **10**, 6051 (1998).
[16] J.O. Vasseur, P.A. Deymier, B. Chenni, B. Djafari-Rouhani, L. Dobrzynski, and D. Prevost, Phys. Rev. Lett. **86**, 3012 (2001).
[17] For a review of this method see M.S. Kuswaha, Recent Res. Devel. Appl. Phys. **2**, 743 (1999).
[18] M. Kafesaki and E.N. Economou, Phys. Rev. B **60**, 11 993 (1999).
[19] Z. Liu, C.T. Chan, P. Sheng, A.L. Goertzen, and J.H. Page, Phys. Rev. B **62**, 2446 (2000).
[20] Y.Y. Chen and Z. Ye, Phys. Rev. E **64**, 036616 (2001); Phys. Rev. Lett. **87**, 184301 (2001).
[21] M. Kafesaki, E. N. Economou, and M. M. Sigalas, *Photonic Band Gap Materials*, edited by C. M. Soukoulis (Kluwer Academic Publishers, The Netherlands, 1996), p. 143.
[22] M. Sigalas and N. García, J. Appl. Phys. **87**, 3122 (2000).
[23] Y. Tanaka, Y. Tomoyasu, and S.I. Tamura, Phys. Rev. B **62**, 7387 (2000).
[24] C. Goffaux, Ph.D. thesis, Presses universitaires de Namur, Namur, 2002.

[25] L. Sanchis, A. Hakansson, F. Cervera, and J. Sánchez-Dehesa, Phys. Rev. B **67**, 035422 (2003).
[26] Z. Liu, X. Zhang, Y. Mao, Y.Y. Zhu, Z. Yang, C.T. Chan, and Ping Sheng, Science **289**, 1734 (2000).
[27] Z. Liu, C.T. Chan, and P. Cheng, Phys. Rev. B **65**, 165116 (2002).
[28] J. Pendry, J. Mod. Opt. **41**, 209 (1994).
[29] C. Goffaux, J. Sánchez-Dehesa, A.L. Yeyati, Ph. Lambin, A. Khelif, J.O. Vasseur, and B. Djafari-Rouhani, Phys. Rev. Lett. **88**, 225502 (2002).
[30] C. de Boor, *Practical Guide to Splines* (Springer, New York, 1978).
[31] E.N. Economou and M.M. Sigalas, J. Acoust. Soc. Am. **95**, 1734 (1994).
[32] J.O. Vasseur and P.A. Deymier, J. Mater. Res. **12**, 2207 (1997).
[33] See, for example, the classical book by L. Brillouin, *Wave Propagation in Periodic Structures* (Dover, New York, 1953).
[34] J.H. Vincent, Philos. Mag. **46**, 557 (1898).